Nanoscale electrochemistry of sp2 carbon materials: from graphite and graphene to carbon nanotubes

Unwin, Patrick R.; G. Guell, Aleix; Zhang, Guohui

Published in:
Accounts of Chemical Research

DOI:
10.1021/acs.accounts.6b00301

Publication date:
2016

Document Version
Peer reviewed version

Nanoscale Electrochemistry of sp^2 Carbon Materials: From Graphite and Graphene to Carbon Nanotubes

Patrick R. Unwin,† Aleix G. Güell,†‡ and Guohui Zhang†*

† Department of Chemistry, University of Warwick, Coventry, CV4 7AL, United Kingdom

‡ School of Engineering and Built Environment, Glasgow Caledonian University, Glasgow, G4 0BA, United Kingdom

* Email: p.r.unwin@warwick.ac.uk

CONSPECTUS

Carbon materials have a long history of use as electrodes in electrochemistry, from (bio)electroanalysis to applications in energy technologies, such as batteries and fuel cells. With the advent of new forms of nano-carbon, particularly carbon nanotubes and graphene, carbon electrode materials have taken on even greater significance for electrochemical studies, both in their own right, and as components and supports in an array of functional composites.

With the increasing prominence of carbon nanomaterials in electrochemistry, comes a need to critically evaluate the experimental framework from which a microscopic understanding of electrochemical processes is best developed. This article advocates the use of emerging electrochemical imaging techniques and confined electrochemical cell formats that have considerable potential to reveal major new perspectives on the intrinsic electrochemical activity of carbon materials, with unprecedented detail and spatial resolution. These techniques allow particular features on a surface to be targeted and models of structure-activity to be developed and tested on a wide range of length scales and time scales.

When high resolution electrochemical imaging data are combined with information from other microscopy and spectroscopy techniques applied to the same area of an electrode surface, in a *correlative-electrochemical microscopy* approach, highly resolved and unambiguous pictures of electrode activity are revealed that provide new views of the electrochemical properties of carbon materials. With a focus on major sp^2 carbon materials – graphite, graphene and single walled carbon nanotubes (SWNTs) – this article summarizes recent advances that have changed understanding of interfacial electrochemistry at carbon electrodes including:

(i) Unequivocal evidence for the high activity of the basal surface of highly oriented pyrolytic graphite (HOPG), which is at least as active as noble metal electrodes (e.g. platinum) for outer-sphere redox processes.

(ii) Demonstration of the high activity of basal plane HOPG towards other reactions, with no requirement for catalysis by step edges or defects, as exemplified by studies of proton-coupled electron transfer, redox transformations of adsorbed molecules, surface functionalization via diazonium electrochemistry and metal electrodeposition.

(iii) Rationalization of the complex interplay of different factors that determine electrochemistry at graphene, including the source (mechanical exfoliation from graphite vs. graphene grown by chemical vapor deposition), number of graphene layers, edges, electronic structure, redox couple, and electrode history effects.

(iv) New methodologies that allow nanoscale electrochemistry of 1D materials (SWNTs) to be related to their electronic characteristics (metallic vs. semiconductor SWNTs), size and quality, with high resolution imaging revealing the high activity of SWNT sidewalls and the importance of defects for some electrocatalytic reactions (e.g. the oxygen reduction reaction).

The experimental approaches highlighted for carbon electrodes are generally applicable to other electrode materials, and set a new framework and course for the study of electrochemical and interfacial processes.

1. INTRODUCTION

Carbon materials can exhibit significant changes in local electronic properties associated with subtle structural variances.[1-4] A longstanding question in electrochemistry is whether the electronic properties of electrodes influence the kinetics of electron transfer,[5-7] with studies of sp^2 carbon materials being important because they have a much lower density of electronic states (DOS) than metal electrodes. For electrocatalytic processes, surface structure and electronic effects must be considered and require careful experimental design.[8]

For graphene and graphite (Figure 1a), the number of graphene layers,[3,9] and the stacking order, have a significant impact on the local electronic structure as seen, for example, in scanning tunneling microscopy (STM) images of graphene (Figure 1b). Furthermore, the DOS, as measured by scanning tunneling spectroscopy (STS), increases monotonically from single layer graphene (SLG) to graphite (Figure 1c). Step edges also need to be considered: those with an armchair configuration (the overwhelming majority) have a similar electronic structure to the basal surface, but zigzag edges have an enhanced DOS at the intrinsic Fermi level (Figure 1d).[1,2,10] SWNTs have a range of possible chirality and defect structures (Figure 1a) that influence the electronic properties (Figure 1e).

Given the heterogeneity in structure and electronic properties, reliable models for the electrochemistry of sp^2 carbon materials can only be obtained through studies that either access particular features (e.g. SWNT sidewalls, SWNT ends, graphene/graphite basal plane, step edges, and defects), or through larger scale measurements where the type and quantity of these structural motifs are thoroughly characterized and systematically varied. In this respect, the use of atomic force microscopy (AFM),[11] STM,[1] micro-Raman spectroscopy[2,12] and other techniques is mandatory. A theme we develop herein is the importance of correlative-electrochemical microscopy, where localized electrochemistry data are combined with complementary microscopy measurements in the same region of a sample, to reveal unambiguous information on electrode structure and electronic controls of electrochemistry.

2. ELECTROCHEMISTRY OF HIGHLY ORIENTED PYROLYTIC GRAPHITE (HOPG) AT THE NANOSCALE

In this section we highlight recent experimental approaches that provide major new insights on sp^2 carbon electrode activity, and allow the development and testing of multiscale (nanoscale to macroscale) models of HOPG electrochemistry. These studies are essential in providing a baseline understanding for other forms of sp^2 carbon.

2.1 Outer-sphere Redox Processes

The most important question concerning HOPG electrochemistry in recent years has been: does the basal surface, free from the influence of step edges, have any (significant) activity or does electrochemistry only occur at step edges? There had been widely differing views, even for outer-sphere redox processes,[11,13,14] where the redox couple does not interact strongly with the electrode surface, but recent high resolution imaging data provide irrefutable evidence for the high activity of the basal surface.

We introduced the scanning micropipet contact method (SMCM), to probe the electroactivity of tiny regions of an HOPG surface, defined by meniscus contact with an electrolyte solution in a micropipet or nanopipet, containing a quasi-reference counter electrode (QRCE).[15] For these studies, the pipet size (ca. 580 nm) was smaller than the inter-step spacing on the basal surface (ca. 2 μm). In the case of the one-electron oxidation of (ferrocenylmethyl)trimethylammonium ($FcTMA^+$), experimental data revealed Nernstian (reversible) electron transfer (ET). A similar, fast ET response was found for $Fe(CN)_6^{4-/3-}$, but measurements had to be made rapidly following HOPG cleavage, to avoid a deterioration of the response.[15]

Although SMCM can now be used with pipets as small as 100 nm diameter,[16] scanning electrochemical cell microscopy (SECCM)[17], as reviewed elsewhere,[18] is a much more powerful method for visualizing electroactivity, because it tracks both surface activity and topography. In the case of HOPG, the response informs on the location of the measurement, i.e., the basal surface

alone, or intersected by step edge(s).[19] The probe is a dual-barrel (theta) nanopipet filled with electrolyte solution that produces a meniscus across the two barrels at the sharp end (Figure 2). This acts as an electrochemical cell upon coming into contact with the substrate of interest. A vertical sinusoidal oscillation is usually imposed on the tip position to create an alternating current (AC) component of the ion conductance current, I_{IC}, due to a bias, V_2, between QRCEs in each barrel, at the oscillation frequency that serves as a feedback parameter to maintain a stable tip-substrate separation while the meniscus is in contact with the surface.[17] The resolution of SECCM approximates to the tip size, which can be as small as 90 nm.[6]

With precise position control of the probe and sample, high-resolution electrochemical imaging (current, I_{EC}, with the working electrode potential controlled by V_1 and V_2; Figure 2) on a variety of substrates is possible.[6,11,12,17,19-22] SECCM imaging was carried out[19] on freshly cleaved HOPG with two redox couples, $Ru(NH_3)_6^{3+/2+}$ and $Fe(CN)_6^{4-/3-}$. High and uniform surface electroactivity was observed across the basal surface (indistinguishable from reversible ET). Lower limits for the standard ET rate constants, $k_0 > 0.5$ cm s^{-1} and > 1 cm s^{-1} were estimated for $Ru(NH_3)_6^{3+/2+}$ and $Fe(CN)_6^{4-/3-}$, respectively,[19] many orders of magnitude higher than previous macroscopic cyclic voltammetry (CV) measurements (by more than 9 orders of magnitude in the case of $Fe(CN)_6^{4-/3-}$).[14,23] For aged HOPG samples exposed to air, both the surface conductivity and the electrochemical response deteriorated, attributed to contamination of the surface and/or delamination of the top layer(s) from the main body of the HOPG.[6,11] These issues need to be considered carefully for the characterization of the intrinsic electrochemical properties of HOPG and exfoliated graphene surfaces.[6,24,25]

Combined scanning electrochemical microscopy (SECM)-AFM,[26,27] likewise enables electroactivity to be directly and simultaneously related to substrate topography, with high spatial resolution.[28,29] It was found[28] that the basal surface of freshly cleaved HOPG was 'as active as template-stripped gold' for $Ru(NH_3)_6^{3+/2+}$ with $k_0 > 9.4$ cm s^{-1}, but that over time (up to several hours) k_0 diminished to 1.9×10^{-2} cm s^{-1}. SECM-AFM measurements on HOPG using a metal-AFM tip functionalized with a tagged

ferrocene-based redox mediator,[30] clearly showed that the basal surface of HOPG displayed high electrochemical activity, although some – but not all – step edges had slightly enhanced currents.[30] In a further study,[31] fully-reversible ET was observed at basal plane HOPG.

High electroactivity of HOPG has been seen in several SECM studies: (i) high resolution imaging studies of the basal surface using the one-electron oxidation of FcMeOH;[32] (ii) in fixed spot measurements with $Fe(CN)_6^{4-/3-}$;[33] and (iii) in nanogaps, for $FcTMA^{+/2+}$,[34] although the adsorption of $FcTMA^{+}$ on HOPG[35] and $FcTMA^{2+}$ on glass[36] needs to be taken into account.

In light of the new views on the nanoscale electrochemical activity of HOPG, macroscopic CV studies have been revisited, with measurements carried out on samples with different (known) step density, under well-defined conditions (e.g. cleavage method, time after cleavage, environment effects), for some of the most studied widely redox couples.[24] Using a simple droplet cell arrangement, in which measurements could be made within a few seconds of HOPG cleavage, CV measurements revealed fast (reversible) ET kinetics, irrespective of step edge density (varied by over 2 orders of magnitude). For both $IrCl_6^{2-/3-}$ ($k_0 > 1.9$ cm s^{-1}) and $Fe(CN)_6^{4-/3-}$ ($k_0 > 0.46$ cm s^{-1}), ET was at least as fast on HOPG as on Pt electrodes, and for $Ru(NH_3)_6^{3+/2+}$ ($k_0 > 0.61$ cm s^{-1}), ET was also fast. Given the considerable difference in DOS between graphite and metal electrodes (see section 1), these results suggest that the DOS of the electrode does not play an important role in the ET kinetics of these outer-sphere redox couples over the range of values encompassing freshly cleaved HOPG and metals.

2.2 Complex Multi-Step Reactions: Neurotransmitter Oxidation

Studies of the electrochemical oxidation of catecholamines on HOPG have demonstrated that the process is neither slow nor solely catalyzed by graphite step edges,[33,37-39] as had previously been proposed.[40] Rather, the electro-oxidation of catecholamines on the basal surface of HOPG is facile. SECCM 'reactive patterning' studies translated the SECCM meniscus across an HOPG surface at a sufficient rate to deduce the response of the fresh surface, but leaving behind polymeric products

that acted as a surface marker.[38,39] This allowed the electrochemical activity to be related directly to the local surface character at the nanoscale by the subsequent use of complementary microscopy in the same area.[39]

Nanoscale measurements predicted that macroscopic CV measurements of catecholamine electro-oxidation would be dominated by the basal surface, which was confirmed in studies of dopamine and epinephrine electro-oxidation.[37-39] An independent SECM study on the redox behavior of dopamine/dopaminequinone on HOPG, also found fast ET characteristics.[33] These studies are important for the design of optimal carbon electrodes for sensing. The low interfacial capacitance of graphite basal electrode surfaces, and the fact that the oxidation reaction occurs easily, lead to far superior concentration detection limits, compared to other carbon electrode materials.[37]

2.3 Adsorbed Systems and Surface Functionalization

The electrochemistry of adsorbed organic molecules had been proposed as an indirect means of characterizing the quality of HOPG surfaces, with quinones, such as adsorbed anthraquinone-2,6-disulfonate (AQDS) considered to only be electroactive at step edges.[23,41] We tested this supposition, using a combination of electrochemical measurements,[42] and found no correlation between the surface coverage of electroactive AQDS and step edge density of HOPG surface.

High resolution electrochemical measurements were performed with an innovative fast scan cyclic voltammetry (FSCV)-SECCM platform (Figure 3a). This revealed the evolution of adsorbed electroactive AQDS on HOPG (Figure 3b and c). The SECCM meniscus was brought into contact with HOPG for defined periods: a hold time (Figure 3a), where the HOPG substrate potential was fixed; and an analysis time, where the potential was scanned at 100 V s^{-1} to record a CV for AQDS reduction and reoxidation (Figure 3b), to determine the amount adsorbed. Step edge density had no influence on the adsorption process, which was dominated by the basal surface, and controlled entirely by AQDS diffusion to the surface (simulation result for this model fitted to the data in Figure

3c). AFM imaging of the areas probed by SECCM (Figure 3d), further revealed no correlation between the fractional coverage of adsorbed electroactive AQDS and the step edge density. The amount of AQDS adsorption was at least 2 orders of magnitude higher than could be accounted for considering only step edges as the adsorption sites for electroactive material (Figure 3e). Kinetic measurements with FSCV-SECCM revealed essentially identical voltammetric behavior on HOPG samples with step edge density that was more than 2 orders magnitude different.[42] Thus: (i) step edges are not required to catalyze ET to adsorbed AQDS on HOPG; and (ii) the reaction is in an adiabatic regime, independent of the DOS.

The grafting of diazonium radicals on carbon electrodes is a popular method for surface modification and there has been debate as to whether it proceeds more readily (and exclusively) at defect sites (step edges and defects),[43,44] and whether it involves covalent modification at all.[45] We studied the reduction of carboxybenzenediazonium in aqueous solution and found that the electrochemistry and modification were independent of step edge density.[46] Moreover, with SECCM we were able to confine the electrochemical modification to isolate the contribution of the basal plane alone, showing unambiguously that step edges were not required for modification. Furthermore, confined electrochemical measurements (1 μm diameter meniscus) allowed us to rule out the need for defect sites, given the low density of point defects on HOPG (between 0.1 and 10 μm^{-2}).[41,47] Covalent modification was proved with micro-Raman spectroscopy[46] and this type of modification has also been demonstrated to proceed readily at defect-free sites at graphene and graphite by STM.[48,49]

2.4 Metal Nucleation and Growth on HOPG

It has often been suggested that step edges are the active sites for metal deposition on graphite and that the atomically smooth basal plane needs to be activated (by some pre-treatment to introduce atomic scale defects)[50] for metal nucleation to occur. However, these findings are usually based on ex-situ characterization of deposited particles, and even in-situ scanned probe microscopy measurements have been unable to capture the initial nucleation events. That nanoparticles (NPs)

are found preferentially at step edges from ex-situ characterization does not necessarily identify the active sites for metal nucleation and growth; instead, it indicates that step sites act to 'anchor' metal NPs.

Using high resolution SECCM, we studied the nucleation of individual Ag NPs on the basal HOPG surface[51] with a meniscus footprint of < 0.2 μm^2, i.e. with no step edges and a very high probability of no point defects. Metal nucleation occurred easily on the basal surface and transient measurements showed the process involved the birth of many nuclei which migrated together (aggregation step) to form a NP which grew to about 25 - 30 nm diameter, before detaching from the surface, in a periodic process with a frequency of a few hundred Hz.

The nucleation-growth-detachment mechanism for metal NP electrodeposition has much in common with the electrochemical aggregative growth model proposed by Ustarroz et al.[52] and which we have further observed in high resolution studies of Pd electrodeposition on HOPG.[53] These studies suggest a need to look beyond the somewhat simplistic classical models for metal nucleation and growth, and indicate the importance of unconventional growth mechanisms.

3. GRAPHENE

Although there is a vast literature on 'graphene' electrochemistry, it mainly concerns reduced graphene oxides and liquid extracted graphene that can be produced and dispersed on a support electrode. Such materials are of variable quality, making fundamental studies difficult.[54] Although there have been interesting high resolution studies on chemical vapor deposition (CVD) graphene,[12,55] exfoliated graphene is of higher quality and so better for fundamental studies. Exfoliated graphene was first investigated by Abruña's group[56] employing an electrochemical cell fabricated by a series of photolithographic steps. The sample, uniquely SLG and with no detectable defects, exhibited high ET kinetics (k_0 > 0.5 cm s^{-1}) for the oxidation of FcMeOH. Dryfe's group produced large exfoliated graphene flakes from Kish graphite (> 100 μm) and investigated the

electrochemistry through two photolithography-free approaches: firstly with resin-based electrochemical cells,[57] and latterly with electrochemical cells defined by micropipet-controlled droplets (20 - 50 μm diameter).[58]

We studied the electrochemistry of two outer-sphere redox couples, $Ru(NH_3)_6^{3+/2+}$ and $FcTMA^{+/2+}$ at exfoliated graphene (Figure 4), using SECCM, which allowed the independent interrogation of different graphene flakes and step edges within the same sample.[6] With the mass transport rates available in SECCM, ET with $FcTMA^{+/2+}$ was found to be fast and reversible on SLG and multilayer graphene. The results with $Ru(NH_3)_6^{3+/2+}$ were more interesting, because the standard potential is close to the intrinsic Fermi level of graphene/graphite (Figure 1e),[59] where the DOS is low, and for graphene is theoretically zero. For this redox couple, there was a strong dependence of the ET kinetics on the number of graphene layers, with SLG having the lowest rate. There was enhanced activity at some, but not all, step edges (Figure 4c,d). The effect was subtle and complementary studies of HOPG showed that this contrast developed with time.[6] We have proposed that spontaneous delamination[6,11] occurring with time leads to a surface made of electronically decoupled regions that are SLG, few-layer and multilayer graphene on top of otherwise intact HOPG. As a consequence, it becomes understandable why, for $Ru(NH_3)_6^{3+/2+}$ in particular, SECCM images feature enhanced currents at exposed step edges (Figure 4d,e), where the apparent rate constant scales with overall step height (Figure 4e,f).

To elucidate the behavior at edges, we developed voltammetric-SECCM[6] where a local CV was recorded at each pixel in an electrochemical image. These measurements established that the voltammetric response at the basal surface and edges were closely similar in shape, but with a small additional overpotential for the basal surface. With $Ru(NH_3)_6^{3+/2+}$, the local electronic structure of graphene becomes a limiting factor in the overall ET rate, leading to a dependency of the observed kinetics on the number of (graphene) layers and step edges.

4. SINGLE WALLED CARBON NANOTUBES

Fundamental studies of SWNTs have focused on high spatial resolution measurements on high quality material (low defect density and low or no metal NP content) grown by catalytic CVD (cCVD) as a forest,[60] or a 2D network[20] or individual SWNT[21,22,61-63] on an otherwise inert Si/SiO_2 substrate. These studies have provided unequivocal evidence that SWNT sidewalls have high electrochemical activity for outer-sphere redox couples for which the ET kinetics can be just as fast as at Pt electrodes.

In order to compare the behavior of metallic and semiconductor SWNTs and to access the activity of different parts of these 1D materials, we developed the platform depicted in Figure 5a, based on flow-aligned SWNTs grown via cCVD onto an insulating Si/SiO_2 substrate.[21,22,62] The catalyst was deposited on one side of the substrate, from where the SWNTs grew, to which a macroscopic Pd electrical contact was applied. The SWNTs were marked at the other end using localized silver electrodeposition, to aid microscopic visualization, leaving a portion of an individual pristine SWNT a few hundred microns long that could be investigated by a range of complementary techniques (Figure 5a). Of particular note is the possibility of measuring electrical conductance current (*I*)-voltage (*V*) by establishing a second moveable electrical contact.

This platform enabled the detailed characterization of SWNT electrochemistry at the nanoscale, which was related to the structural and electronic properties of the SWNT. The example data in Figure 5b,c highlights that SWNT sidewalls are more or less uniformly active for outer-sphere redox processes.[21] SWNTs with metallic character showed kinetics similar to metal electrodes, but semiconductor SWNTs showed behavior dependent on the formal potential of the redox couple. The standard potential of the $Ru(NH_3)_6^{3+/2+}$ couple lies in the charge depletion region of semiconductor SWNTs which largely shuts off the redox reaction.[63]

SECCM also revealed the sidewalls of SWNTs to be electroactive for some inner-sphere processes, with O_2 reduction to H_2O_2 being just as fast on the straight sidewalls of SWNTs as on standard gold electrocatalysts, but with a great enhancement in activity at kink sites (Figure 5d).[22] At very low

driving force, defects also appear to be the sites for metal NP growth,[64] and can be used to decorate such sites, although as we pointed out in section 2.4, the sites where metal NPs are observed signifies the most stable location and not necessarily the site(s) of initial nucleation. At higher driving force, SWNTs are highly active towards metal electrodeposition and metal nanowires can be produced using SWNTs as a template.[65,66]

5. CONCLUSIONS

An overreliance on classical macroscopic approaches to derive microscopic electrochemistry models of carbon electrodes, resulted in important features of electrochemical processes being obscured or misinterpreted. This article has advocated radical fresh approaches and, in particular, sought to demonstrate how correlative-electrochemical microscopy is particularly powerful in providing major new perspectives on electrochemical processes at the nanoscale. The advances described provide a new framework on the activity of carbon electrode materials, which will direct future use in sensing and energy applications (among others). From a fundamental viewpoint, this article has highlighted that while the DOS (and electronic structure) of certain carbon materials (e.g. graphene and semiconductor carbon nanotubes) may be important in determining electron transfer kinetics for some redox reactions, it does not for others, and graphite itself behaves like a metal for many electrode reactions, with the basal surface being highly active towards a wide range of electrochemical processes.

ACKNOWLEDGEMENTS

We deeply appreciate the outstanding contributions of many colleagues to Warwick's programme on carbon electrodes, and are grateful to the European Union, the EPSRC and the University of Warwick for generous support.

Biographical Information

Patrick Unwin is a graduate of the universities of Liverpool (BSc), Oxford (DPhil) and Warwick (DSc). He founded the Electrochemistry & Interfaces Group at the University of Warwick, where he has been Professor since 1998. His interests are in instrumentation development and application to interfacial processes.

Aleix Güell received his PhD in Chemistry from the University of Barcelona. He is presently a lecturer at Glasgow Caledonian University. His main interests include synthesis and applications of nanomaterials, SPM instrumentation and nanoscale phenomena.

Guohui Zhang received his bachelor and master degrees from Shandong University, China, in 2010 and 2012. He is presently pursuing his Ph.D. degree at the University of Warwick, under the supervision of Patrick Unwin, on the electrochemistry of carbon materials.

REFERENCES

(1) Niimi, Y.; Matsui, T.; Kambara, H.; Tagami, K.; Tsukada, M.; Fukuyama, H. Scanning Tunneling Microscopy and Spectroscopy of the Electronic Local Density of States of Graphite Surfaces near Monoatomic Step Edges. *Phys. Rev. B* **2006**, *73*, 085421.

(2) Nakada, K.; Fujita, M.; Dresselhaus, G.; Dresselhaus, M. S. Edge State in Graphene Ribbons: Nanometer Size Effect and Edge Shape Dependence. *Phys. Rev. B* **1996**, *54*, 17954-17961.

(3) Partoens, B.; Peeters, F. M. From Graphene to Graphite: Electronic Structure around the K Point. *Phys. Rev. B* **2006**, *74*, 075404.

(4) Kondo, T.; Honma, Y.; Oh, J.; Machida, T.; Nakamura, J. Edge States Propagating from a Defect of Graphite: Scanning Tunneling Spectroscopy Measurements. *Phys. Rev. B* **2010**, *82*, 153414.

(5) Chen, S.; Liu, Y.; Chen, J. Heterogeneous Electron Transfer at Nanoscopic Electrodes: Importance of Electronic Structures and Electric Double Layers. *Chem. Soc. Rev.* **2014**, *43*, 5372-5386.

(6) Güell, A. G.; Cuharuc, A. S.; Kim, Y. R.; Zhang, G.; Tan, S. Y.; Ebejer, N.; Unwin, P. R. Redox-Dependent Spatially Resolved Electrochemistry at Graphene and Graphite Step Edges. *ACS Nano* **2015**, *9*, 3558-3571.

(7) Schmickler, W.; Santos, E.: *Interfacial Electrochemistry*; 2 ed.; Springer-Verlag Berlin Heidelberg, 2010.

(8) Kleijn, S. E. F.; Lai, S. C. S.; Koper, M. T. M.; Unwin, P. R. Electrochemistry of Nanoparticles. *Angew. Chem. Int. Ed.* **2014**, *53*, 3558-3586.

(9) Li, G.; Luican, A.; Andrei, E. Y. Scanning Tunneling Spectroscopy of Graphene on Graphite. *Phys. Rev. Lett.* **2009**, *102*, 176804.

(10) Kobayashi, Y.; Fukui, K.-i.; Enoki, T.; Kusakabe, K.; Kaburagi, Y. Observation of Zigzag and Armchair Edges of Graphite Using Scanning Tunneling Microscopy and Spectroscopy. *Phys. Rev. B* **2005**, *71*, 193406.

(11) Patel, A. N.; Collignon, M. G.; O'Connell, M. A.; Hung, W. O.; McKelvey, K.; Macpherson, J. V.; Unwin, P. R. A New View of Electrochemistry at Highly Oriented Pyrolytic Graphite. *J. Am. Chem. Soc.* **2012**, *134*, 20117-20130.

(12) Güell, A. G.; Ebejer, N.; Snowden, M. E.; Macpherson, J. V.; Unwin, P. R. Structural Correlations in Heterogeneous Electron Transfer at Monolayer and Multilayer Graphene Electrodes. *J. Am. Chem. Soc.* **2012**, *134*, 7258-7261.

(13) McCreery, R. L.; McDermott, M. T. Comment on Electrochemical Kinetics at Ordered Graphite Electrodes. *Anal. Chem.* **2012**, *84*, 2602-2605.

(14) Banks, C. E.; Davies, T. J.; Wildgoose, G. G.; Compton, R. G. Electrocatalysis at Graphite and Carbon Nanotube Modified Electrodes: Edge-Plane Sites and Tube Ends Are the Reactive Sites. *Chem. Commun.* **2005**, 829-841.

(15) Williams, C. G.; Edwards, M. A.; Colley, A. L.; Macpherson, J. V.; Unwin, P. R. Scanning Micropipet Contact Method for High-Resolution Imaging of Electrode Surface Redox Activity. *Anal. Chem.* **2009**, *81*, 2486-2495.

(16) Takahashi, Y.; Kumatani, A.; Munakata, H.; Inomata, H.; Ito, K.; Ino, K.; Shiku, H.; Unwin, P. R.; Korchev, Y. E.; Kanamura, K.; Matsue, T. Nanoscale Visualization of Redox Activity at Lithium-Ion Battery Cathodes. *Nat. Commun.* **2014**, *5*, 5450.

(17) Ebejer, N.; Schnippering, M.; Colburn, A. W.; Edwards, M. A.; Unwin, P. R. Localized High Resolution Electrochemistry and Multifunctional Imaging: Scanning Electrochemical Cell Microscopy. *Anal. Chem.* **2010**, *82*, 9141-9145.

(18) Ebejer, N.; Guell, A. G.; Lai, S. C.; McKelvey, K.; Snowden, M. E.; Unwin, P. R. Scanning Electrochemical Cell Microscopy: A Versatile Technique for Nanoscale Electrochemistry and Functional Imaging. *Annu. Rev. Anal. Chem.* **2013**, *6*, 329-351.

(19) Lai, S. C. S.; Patel, A. N.; McKelvey, K.; Unwin, P. R. Definitive Evidence for Fast Electron Transfer at Pristine Basal Plane Graphite from High-Resolution Electrochemical Imaging. *Angew. Chem. Int. Ed.* **2012**, *51*, 5405-5408.

(20) Güell, A. G.; Ebejer, N.; Snowden, M. E.; McKelvey, K.; Macpherson, J. V.; Unwin, P. R. Quantitative Nanoscale Visualization of Heterogeneous Electron Transfer Rates in 2D Carbon Nanotube Networks. *Proc. Natl. Acad. Sci. U. S. A.* **2012**, *109*, 11487-11492.

(21) Güell, A. G.; Meadows, K. E.; Dudin, P. V.; Ebejer, N.; Macpherson, J. V.; Unwin, P. R. Mapping Nanoscale Electrochemistry of Individual Single-Walled Carbon Nanotubes. *Nano Lett.* **2014**, *14*, 220-224.

(22) Byers, J. C.; Güell, A. G.; Unwin, P. R. Nanoscale Electrocatalysis: Visualizing Oxygen Reduction at Pristine, Kinked, and Oxidized Sites on Individual Carbon Nanotubes. *J. Am. Chem. Soc.* **2014**, *136*, 11252-11255.

(23) McDermott, M. T.; Kneten, K.; McCreery, R. L. Anthraquinonedisulfonate Adsorption, Electron-Transfer Kinetics, and Capacitance on Ordered Graphite Electrodes: The Important Role of Surface Defects. *J. Phys. Chem.* **1992**, *96*, 3124-3130.

(24) Zhang, G.; Cuharuc, A. S.; Güell, A. G.; Unwin, P. R. Electrochemistry at Highly Oriented Pyrolytic Graphite (HOPG): Lower Limit for the Kinetics of Outer-sphere Redox Processes and General Implications for Electron Transfer Models. *Phys. Chem. Chem. Phys.* **2015**, *17*, 11827-11838.

(25) Li, Z.; Kozbial, A.; Nioradze, N.; Parobek, D.; Shenoy, G. J.; Salim, M.; Amemiya, S.; Li, L.; Liu, H. Water Protects Graphitic Surface from Airborne Hydrocarbon Contamination. *ACS Nano* **2016**, *10*, 349-359.

(26) Macpherson, J. V.; Unwin, P. R. Combined Scanning Electrochemical–Atomic Force Microscopy. *Anal. Chem.* **2000**, *72*, 276-285.

(27) Kranz, C.; Friedbacher, G.; Mizaikoff, B.; Lugstein, A.; Smoliner, J.; Bertagnolli, E. Integrating an Ultramicroelectrode in an AFM Cantilever: Combined Technology for Enhanced Information. *Anal. Chem.* **2001**, *73*, 2491-2500.

(28) Frederix, P. L.; Bosshart, P. D.; Akiyama, T.; Chami, M.; Gullo, M. R.; Blackstock, J. J.; Dooleweerdt, K.; de Rooij, N. F.; Staufer, U.; Engel, A. Conductive Supports for Combined AFM-SECM on Biological Membranes. *Nanotechnology* **2008**, *19*, 384004.

(29) Wain, A. J.; Pollard, A. J.; Richter, C. High-Resolution Electrochemical and Topographical Imaging Using Batch-Fabricated Cantilever Probes. *Anal. Chem.* **2014**, *86*, 5143-5149.

(30) Anne, A.; Cambril, E.; Chovin, A.; Demaille, C.; Goyer, C. Electrochemical Atomic Force Microscopy Using a Tip-Attached Redox Mediator for Topographic and Functional Imaging of Nanosystems. *ACS Nano* **2009**, *3*, 2927-2940.

(31) Anne, A.; Bahri, M. A.; Chovin, A.; Demaille, C.; Taofifenua, C. Probing the Conformation and 2D-Distribution of Pyrene-Terminated Redox-Labeled Poly(ethylene glycol) Chains End-Adsorbed on HOPG Using Cyclic Voltammetry and Atomic Force Electrochemical Microscopy. *Phys. Chem. Chem. Phys.* **2014**, *16*, 4642-4652.

(32) Sun, T.; Yu, Y.; Zacher, B. J.; Mirkin, M. V. Scanning Electrochemical Microscopy of Individual Catalytic Nanoparticles. *Angew. Chem. Int. Ed.* **2014**, *53*, 14120-14123.

(33) Lhenry, S.; Leroux, Y. R.; Hapiot, P. Use of Catechol As Selective Redox Mediator in Scanning Electrochemical Microscopy Investigations. *Anal. Chem.* **2012**, *84*, 7518-7524.

(34) Nioradze, N.; Chen, R.; Kurapati, N.; Khvataeva-Domanov, A.; Mabic, S.; Amemiya, S. Organic Contamination of Highly Oriented Pyrolytic Graphite As Studied by Scanning Electrochemical Microscopy. *Anal. Chem.* **2015**, *87*, 4836-4843.

(35) Cuharuc, A. S.; Zhang, G.; Unwin, P. R. Electrochemistry of Ferrocene Derivatives on Highly Oriented Pyrolytic Graphite (HOPG): Quantification and Impacts of Surface Adsorption. *Phys. Chem. Chem. Phys.* **2016**, *18*, 4966-4977.

(36) Tan, S.-y.; Zhang, J.; Bond, A. M.; Macpherson, J. V.; Unwin, P. R. Impact of Adsorption on Scanning Electrochemical Microscopy Voltammetry and Implications for Nanogap Measurements. *Anal. Chem.* **2016**, *88*, 3272-3280.

(37) Patel, A. N.; Tan, S. Y.; Miller, T. S.; Macpherson, J. V.; Unwin, P. R. Comparison and Reappraisal of Carbon Electrodes for the Voltammetric Detection of Dopamine. *Anal. Chem.* **2013**, *85*, 11755-11764.

(38) Patel, A. N.; Tan, S. Y.; Unwin, P. R. Epinephrine Electro-Oxidation Highlights Fast Electrochemistry at the Graphite Basal Surface. *Chem. Commun.* **2013**, *49*, 8776-8778.

(39) Patel, A. N.; McKelvey, K.; Unwin, P. R. Nanoscale Electrochemical Patterning Reveals the Active Sites for Catechol Oxidation at Graphite Surfaces. *J. Am. Chem. Soc.* **2012**, *134*, 20246-20249.

(40) McCreery, R. L. Advanced Carbon Electrode Materials for Molecular Electrochemistry. *Chem. Rev.* **2008**, *108*, 2646-2687.

(41) McDermott, M. T.; McCreery, R. L. Scanning Tunneling Microscopy of Ordered Graphite and Glassy Carbon Surfaces: Electronic Control of Quinone Adsorption. *Langmuir* **1994**, *10*, 4307-4314.

(42) Zhang, G.; Kirkman, P. M.; Patel, A. N.; Cuharuc, A. S.; McKelvey, K.; Unwin, P. R. Molecular Functionalization of Graphite Surfaces: Basal Plane versus Step Edge Electrochemical Activity. *J. Am. Chem. Soc.* **2014**, *136*, 11444-11451.

(43) Kariuki, J. K.; McDermott, M. T. Nucleation and Growth of Functionalized Aryl Films on Graphite Electrodes. *Langmuir* **1999**, *15*, 6534-6540.

(44) Allongue, P.; Delamar, M.; Desbat, B.; Fagebaume, O.; Hitmi, R.; Pinson, J.; Savéant, J.-M. Covalent Modification of Carbon Surfaces by Aryl Radicals Generated from the Electrochemical Reduction of Diazonium Salts. *J. Am. Chem. Soc.* **1997**, *119*, 201-207.

(45) Ma, H.; Lee, L.; Brooksby, P. A.; Brown, S. A.; Fraser, S. J.; Gordon, K. C.; Leroux, Y. R.; Hapiot, P.; Downard, A. J. Scanning Tunneling and Atomic Force Microscopy Evidence for Covalent and Noncovalent Interactions between Aryl Films and Highly Ordered Pyrolytic Graphite. *J. Phys. Chem. C* **2014**, *118*, 5820-5826.

(46) Kirkman, P. M.; Güell, A. G.; Cuharuc, A. S.; Unwin, P. R. Spatial and Temporal Control of the Diazonium Modification of sp^2 Carbon Surfaces. *J. Am. Chem. Soc.* **2014**, *136*, 36-39.

(47) Chang, H.; Bard, A. J. Scanning Tunneling Microscopy Studies of Carbon-Oxygen Reactions on Highly Oriented Pyrolytic Graphite. *J. Am. Chem. Soc.* **1991**, *113*, 5588-5596.

(48) Greenwood, J.; Phan, T. H.; Fujita, Y.; Li, Z.; Ivasenko, O.; Vanderlinden, W.; Van Gorp, H.; Frederickx, W.; Lu, G.; Tahara, K.; Tobe, Y.; Uji-i, H.; Mertens, S. F. L.; De Feyter, S. Covalent Modification of Graphene and Graphite Using Diazonium Chemistry: Tunable Grafting and Nanomanipulation. *ACS Nano* **2015**, *9*, 5520-5535.

(49) Stevenson, K. J.; Veneman, P. A.; Gearba, R. I.; Mueller, K. M.; Holliday, B. J.; Ohta, T.; Chan, C. K. Controlled Covalent Modification of Epitaxial Single Layer Graphene on 6H-SiC (0001) with Aryliodonium Salts Using Electrochemical Methods. *Faraday Discuss.* **2014**, *172*, 273-291.

(50) Zoval, J. V.; Stiger, R. M.; Biernacki, P. R.; Penner, R. M. Electrochemical Deposition of Silver Nanocrystallites on the Atomically Smooth Graphite Basal Plane. *J. Phys. Chem.* **1996**, *100*, 837-844.

(51) Lai, S. C. S.; Lazenby, R. A.; Kirkman, P. M.; Unwin, P. R. Nucleation, Aggregative Growth and Detachment of Metal Nanoparticles during Electrodeposition at Electrode Surfaces. *Chem. Sci.* **2015**, *6*, 1126-1138.

(52) Ustarroz, J.; Hammons, J. A.; Altantzis, T.; Hubin, A.; Bals, S.; Terryn, H. A Generalized Electrochemical Aggregative Growth Mechanism. *J. Am. Chem. Soc.* **2013**, *135*, 11550-11561.

(53) Kim, Y.-R.; Lai, S. C. S.; McKelvey, K.; Zhang, G.; Perry, D.; Miller, T. S.; Unwin, P. R. Nucleation and Aggregative Growth of Palladium Nanoparticles on Carbon Electrodes: Experiment and Kinetic Model. *J. Phys. Chem. C* **2015**, *119*, 17389-17397.

(54) Patten, H. V.; Velický, M.; Dryfe, R. A. W.: Electrochemistry of Graphene. In *Electrochemistry of Carbon Electrodes*; Wiley-VCH Verlag GmbH & Co. KGaA, 2015; pp 121-162.

(55) Zhong, J.-H.; Zhang, J.; Jin, X.; Liu, J.-Y.; Li, Q.; Li, M.-H.; Cai, W.; Wu, D.-Y.; Zhan, D.; Ren, B. Quantitative Correlation between Defect Density and Heterogeneous Electron Transfer Rate of Single Layer Graphene. *J. Am. Chem. Soc.* **2014**, *136*, 16609-16617.

(56) Li, W.; Tan, C.; Lowe, M. A.; Abruña, H. D.; Ralph, D. C. Electrochemistry of Individual Monolayer Graphene Sheets. *ACS Nano* **2011**, *5*, 2264-2270.

(57) Valota, A. T.; Kinloch, I. A.; Novoselov, K. S.; Casiraghi, C.; Eckmann, A.; Hill, E. W.; Dryfe, R. A. W. Electrochemical Behavior of Monolayer and Bilayer Graphene. *ACS Nano* **2011**, *5*, 8809-8815.

(58) Velický, M.; Bradley, D. F.; Cooper, A. J.; Hill, E. W.; Kinloch, I. A.; Mishchenko, A.; Novoselov, K. S.; Patten, H. V.; Toth, P. S.; Valota, A. T.; Worrall, S. D.; Dryfe, R. A. W. Electron Transfer Kinetics on Mono- and Multilayer Graphene. *ACS Nano* **2014**, *8*, 10089-10100.

(59) Kneten, K. R.; McCreery, R. L. Effects of Redox System Structure on Electron-Transfer Kinetics at Ordered Graphite and Glassy Carbon Electrodes. *Anal. Chem.* **1992**, *64*, 2518-2524.

(60) Miller, T. S.; Ebejer, N.; Guell, A. G.; Macpherson, J. V.; Unwin, P. R. Electrochemistry at Carbon Nanotube Forests: Sidewalls and Closed Ends Allow Fast Electron Transfer. *Chem. Commun.* **2012**, *48*, 7435-7437.

(61) Corso, B. L.; Perez, I.; Sheps, T.; Sims, P. C.; Gül, O. T.; Collins, P. G. Electrochemical Charge-Transfer Resistance in Carbon Nanotube Composites. *Nano Lett.* **2014**, *14*, 1329-1336.

(62) Güell, A. G.; Meadows, K. E.; Dudin, P. V.; Ebejer, N.; Byers, J. C.; Macpherson, J. V.; Unwin, P. R. Selection, Characterisation and Mapping of Complex Electrochemical Processes at Individual Single-Walled Carbon Nanotubes: The Case of Serotonin Oxidation. *Faraday Discuss.* **2014**, *172*, 439-455.

(63) Heller, I.; Kong, J.; Williams, K. A.; Dekker, C.; Lemay, S. G. Electrochemistry at Single-Walled Carbon Nanotubes: The Role of Band Structure and Quantum Capacitance. *J. Am. Chem. Soc.* **2006**, *128*, 7353-7359.

(64) Fan, Y.; Goldsmith, B. R.; Collins, P. G. Identifying and Counting Point Defects in Carbon Nanotubes. *Nat. Mater.* **2005**, *4*, 906-911.

(65) Dudin, P. V.; Snowden, M. E.; Macpherson, J. V.; Unwin, P. R. Electrochemistry at Nanoscale Electrodes: Individual Single-Walled Carbon Nanotubes (SWNTs) and SWNT-Templated Metal Nanowires. *ACS Nano* **2011**, *5*, 10017-10025.

(66) Quinn, B. M.; Dekker, C.; Lemay, S. G. Electrodeposition of Noble Metal Nanoparticles on Carbon Nanotubes. *J. Am. Chem. Soc.* **2005**, *127*, 6146-6147.

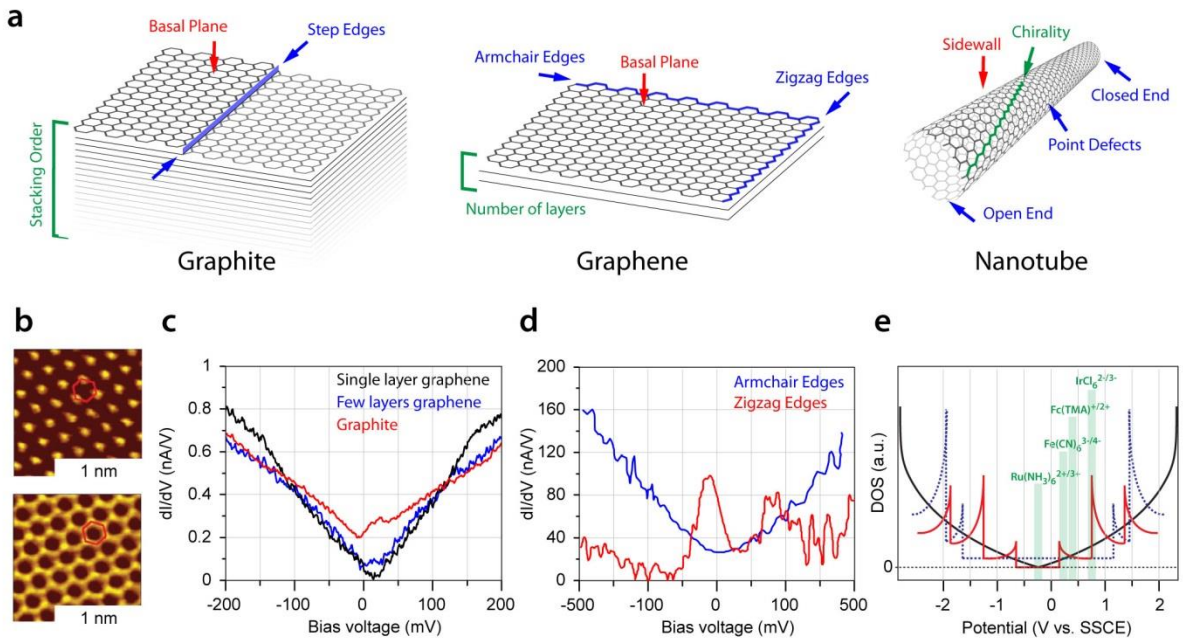

Figure 1. (a) Schematic of sp^2 carbon materials, indicating key intrinsic structural motifs. (b) STM images of few-layer graphene (top) and single layer graphene (bottom). Reproduced with permission from ref.9. Copyright 2009 American Physical Society. (c) and (d) Experimental STS spectra as a function of the number of graphene layers or edge termination. Reproduced with permission from ref.9 and ref.10, respectively. Copyright 2009 and 2005 American Physical Society. (e) Electronic band structure of graphene (solid black line), and exemplar SWNTs (semiconductor, solid red line; metallic, dashed blue line). Reproduced with permission from ref.63. Copyright 2006 American Chemical Society. The position of standard potentials for typical one-electron outer-sphere redox couples is also shown. Reproduced with permission from refs.6 and 59, respectively. Copyright 2015 and 1992 American Chemical Society.

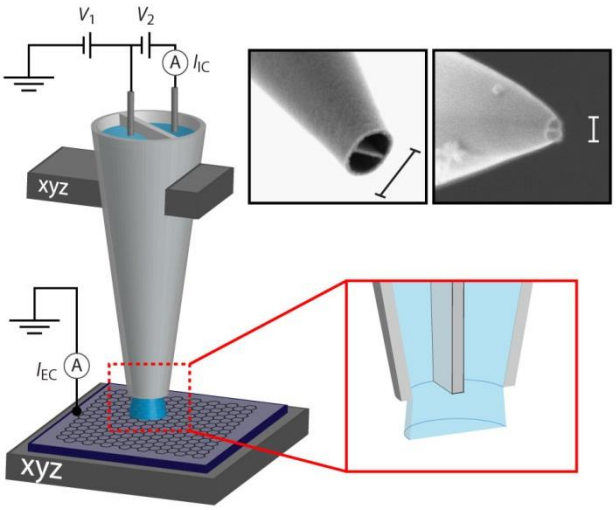

Figure 2. Schematic of the SECCM setup, making use of a nanopipet (example electron microscopy images for pipets of 1 μm and 90 nm diameter shown top right) to confine electrochemical measurements to the tiny meniscus formed between the probe and surface. The pipet is scanned over the surface by means of piezoelectric (*xyz*) positioners, to map electrochemical activity and topography (see text for further details).

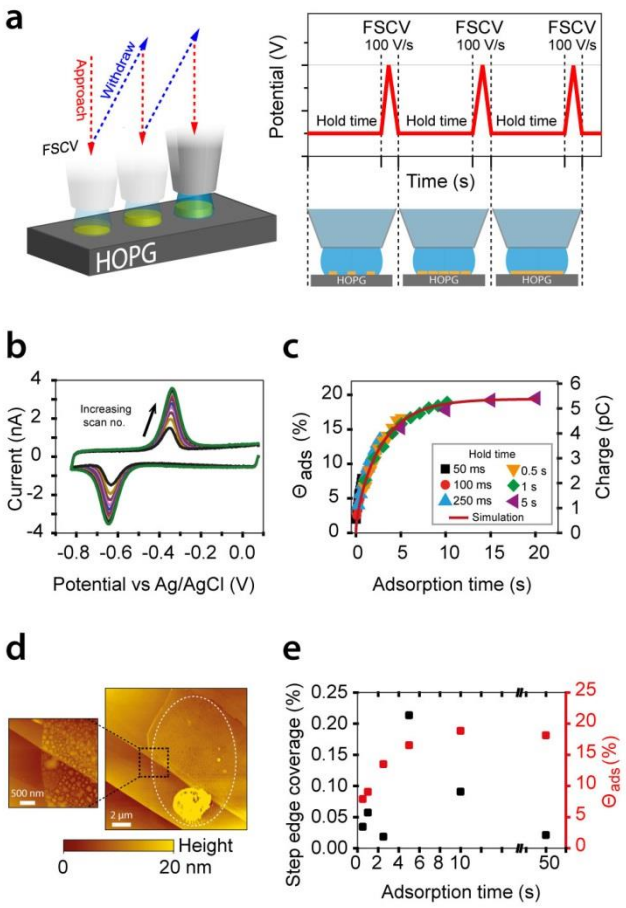

Figure 3. (a) Schematic of the FSCV-SECCM setup where a series of CV scans is carried out in a sequence of spots on an HOPG surface, to monitor AQDS adsorption. (b) 10 FSCVs at 100 V s^{-1} for the adsorption of AQDS (250 ms hold time between measurements), at high quality HOPG. (c) Fractional coverage and corresponding charge for adsorbed AQDS at an HOPG surface as a function of time. Solid line indicates diffusion-controlled adsorption. (d) Typical AFM images (ex-situ) of an adsorption spot on an HOPG surface after about 10 s AQDS adsorption; approximate droplet footprint outlined in white. (e) Percentage of step edges measured by AFM within adsorption spots and the observed fractional coverage of electroactive AQDS for a set of adsorption times. Reproduced with permission from ref.42. Copyright 2014 American Chemical Society.

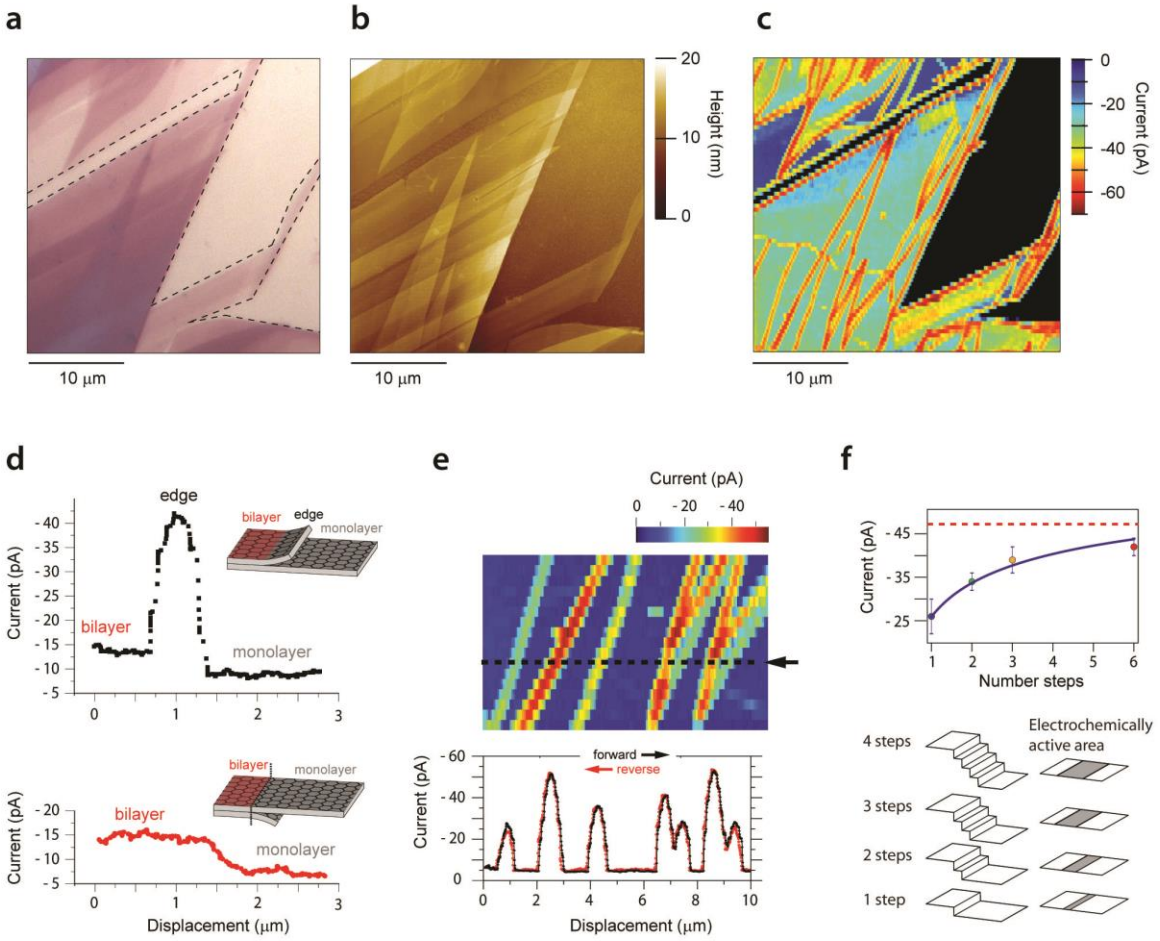

Figure 4. (a) Optical microscopy image, (b) AFM image and (c) SECCM electroactivity map of the reduction of $Ru(NH_3)_6^{3+}$ for the same area of an exfoliated graphene sample on a silicon/silicon oxide substrate. (d) SECCM current scan profiles of two characteristics over step edges: electrochemically active (top) and non-active (bottom) depending on the step edge being exposed or buried. (e) SECCM electroactivity map of step edges of different overall height (from AFM, not shown) and thus different electrochemically active areas (f). Adapted with permission from ref.6. Copyright 2015 American Chemical Society.

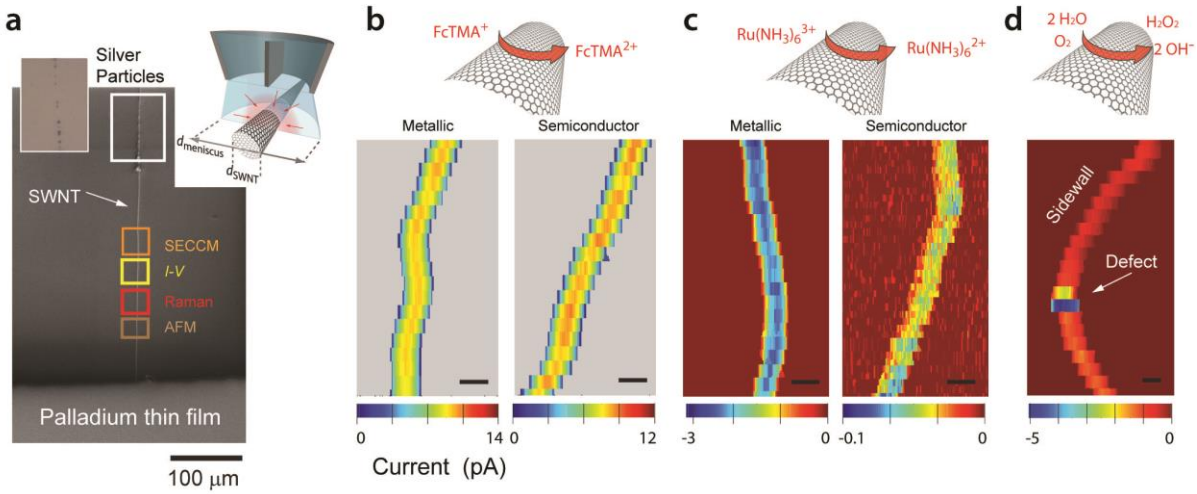

Figure 5. (a) Platform based on individual flow-aligned SWNTs for the correlation of electrochemical activity and structure/properties. Various techniques can be deployed on the same SWNT (e.g. Raman, AFM, SECCM, electrical measurements). (b) and (c) SECCM maps showing the homogeneous activity of SWNT sidewalls for $FcTMA^{+}$ oxidation and $Ru(NH_3)_6^{3+}$ reduction at metallic and semiconductor SWNTs. (d) High resolution SECCM image highlighting the exceptional activity of intrinsic kink defects on nanotubes for oxygen reduction. Scale bar is 500 nm. Reproduced with permission from refs.21 and 22. Copyright 2014 American Chemical Society.

Conspectus Figure